

Optimizing modern radar systems using low-latency, high-performance FFT coprocessors



Dr. June Chul Roh
*Senior Systems Architect,
Embedded Processing*

Dr. Slaheddine Aridhi
*Senior Systems Architect,
Communications Processors*

Texas Instruments

Introduction

Modern radar systems rely greatly on the fast Fourier transform (FFT) and the overall performance of the system is often tied to the efficiency of the FFT processing. TI has developed a high-precision and high-performance FFT coprocessor (FFTC) that can be used to enhance the performance of radar systems, thereby enabling lower power and cost solutions. The FFTC resides on a number of TI multicore system-on-chips (SoCs), including **66AK2L06**, **TCI6636K2H** and **TCI6638K2K** SoCs, which contain both ARM[®] Cortex[®]-A15 cores and C66x digital signal processor (DSP) cores. To put the FFTC performance in perspective, the TCI6638K2K can implement over 4.5 million, 1024-point FFT operations per second using six FFTCs, compared to an equivalent ~300,000 FFTs per second using six C66x DSP cores.

In this paper, we simulate the implementation of a synthetic aperture radar (SAR) system on a TI multicore SoC in order to compare the FFTC performance to single-precision (SP) floating-point FFT implementations and show that there is no appreciable performance loss due to the precision of the FFTC. The results show that radar designers can use the FFTC to offload other cores in the SoC and achieve lower size, weight and power (SWaP) for radar systems. For more information on SAR systems and the use of DSPs for SAR, see [1] and [2].

KeyStone™-based SoC for SAR processing

The 66AK2L06 (shown in Figure 1) is one of the TI KeyStone™ architecture-based SoCs that are ideal for radar signal processing [1]. This SoC has unique features allowing the complete signal processing chain for radar systems to be implemented efficiently. In addition to the processing cores and the FFTC engines, the SoC also contains a JESD204B interface and a digital front end (DFE) processing block. The JESD204B interface allows a direct connection to an analog-to-digital convertor (ADC) and the

DFE engine implements the I/Q mapping, digital down-conversion, FIR filtering and decimation. The resulting baseband data can be processed using the four C66x DSP cores and two FFTCs

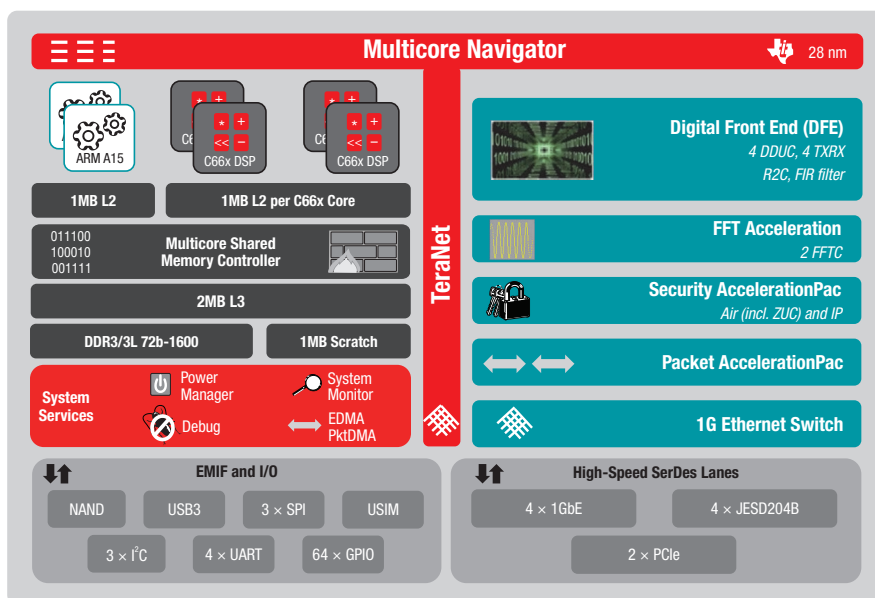


Figure 1: 66AK2L06 SoC block diagram

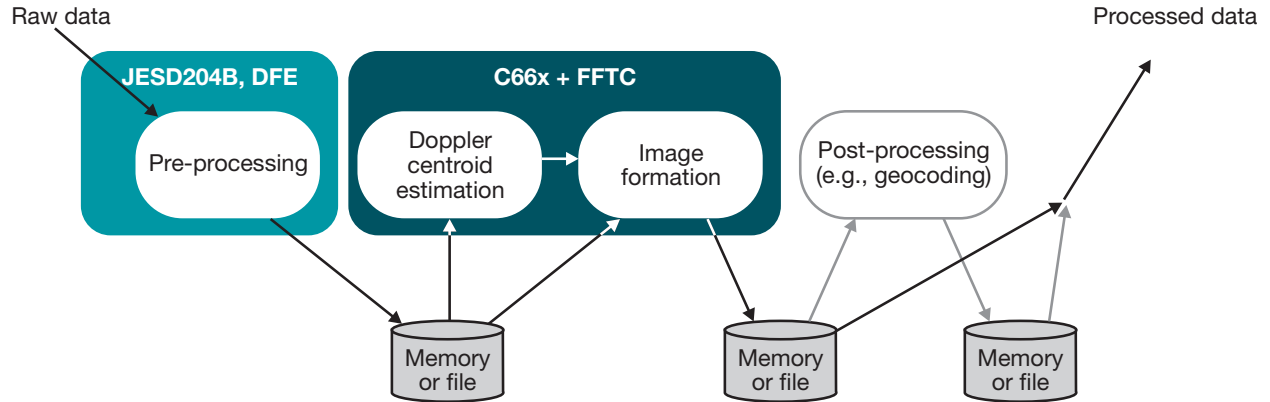


Figure 2: High-level SAR signal processing flow in 66AK2L06 SoC.

for Doppler centroid estimation and SAR image formation. The mapping of functional blocks of the radar signal processing chain is outlined above in Figure 2.

FFTC performance

The FFTC is the hardware module employed to accelerate the FFT and IFFT computations required in various applications such as radar, avionics, test and measurement and wireless systems. Table 1 compares the performance of the FFTC to that of a 32-bit single-precision, floating-point FFT implemented on a C66x DSP core.

| Performance metric | Processing core | FFT Size | | | |
|--------------------|-----------------|----------|---------|---------|--------|
| | | 1024 | 2048 | 4096 | 8192 |
| FFTs per second | FFT coprocessor | 705,000 | 303,000 | 154,000 | 66,000 |
| | C66x DSP core | 74,000 | 35,000 | 9,000 | 4,000 |
| Equivalent GFLOPS | FFT coprocessor | 36.1 | 34.1 | 37.8 | 35.4 |
| | C66x DSP core | 4.5 | 4.2 | 4.5 | 2.5 |
| SNR (dB) | FFT coprocessor | 85.2 | 84.8 | 84.1 | 83.8 |
| | C66x DSP core | ~300 | ~300 | ~300 | ~300 |

Table 1. FFT performance table

The GFLOPS values shown in Table 1 are computed according to the following equation:

$$GFLOPS = \frac{5N \log_2 N}{T}$$

where N is the FFT size and T is the time required for the computation in nanoseconds.

The FFTC throughput is about 10 times that of the SP floating-point FFT implementation on the C66x DSP core. This high throughput can be used to improve the latency as well as the performance of the SAR system. Note also that the signal-to-noise-ratio (SNR) of the FFTC is lower than that of the DSP implementation as the FFTC uses a block floating-point implementation. We will show in the following sections that the SNR of the FFTC is high enough for SAR implementations and that this SNR difference is negligible in terms of overall system performance. One point to note is that the SNR performance of the FFTC is about 20 dB better than the performance of 16-bit fixed-point FFT implementations, which we measured to be in the 63–65 dB range.

FFTC scalability

TI provides a broad, scalable portfolio of real-time, deterministic and easily programmable KeyStone-based devices. These devices not only scale

FFTC features

The FFTC provides the following features:

- The following sizes are allowed:
 - $2^a \times 3^b$ (for $2 \leq a \leq 13$, $0 \leq b \leq 1$), for a maximum size of 8192
 - $12 \times 2^a \times 3^b \times 5^c$ (where a , b , and c are integers), for sizes between 12 and 1296
- 16 bits I / 16 bits Q input and output (internal accuracy is higher)
- SNR ranging from 84 to 100 dB depending on the FFT size
- Dynamic and programmable scaling modes, providing the programmer full flexibility to choose the use of dynamic range at each stage of the FFTC operation
- Dynamic scaling mode which returns block exponents. In this mode, the dynamic range is automatically optimized without user intervention at each stage of FFT operation
- Support for “FFT shift” (switching between left/right halves)
- Support for cyclic prefix (both addition and removal). This is a useful feature in orthogonal frequency division multiplexing (OFDM) based communication systems
- Ping/Pong input and output buffers that allow streaming of data through the FFT engine without incurring overhead when transferring data to and from FFTC
- Additional flexibility in choosing data formats and scaling:
 - Input data scaling with shift
 - Output data scaling
 - Programmable input I/Q data format.
 - Programmable input I/Q data size (16-bit/8-bit)

For a more detailed description of the FFTC, see ^[3].

across DSP and ARM cores but also scale across the number of hardware accelerators, including FFTC hardware accelerator. The FFTC accelerator in these devices is designed for general-purpose

signal-processing applications. Scalable, non-blocking FFTC accelerators fully offload all the FFT operations including the use of overlapping FFT frames, leaving the C66x DSP cores for advanced signal-processing tasks and reducing the overall system latency. Table 2 summarizes TI's portfolio of KeyStone architecture-based devices with the number of FFTC accelerators and FFT performance for each device.

Applying FFTC to SAR signal processing

SAR ^[4] is an air-borne or space-borne, side-looking radar system for generating high-resolution radar imagery in defense and remote-sensing applications. The motion of the SAR platform artificially creates a very large linear antenna array, and the multiple radar echoes, which correspond to the synthetic aperture length, can be coherently-combined to produce high-quality SAR images. These coherent SAR image-formation algorithms rely heavily on FFT processing, implementing the majority of matched filtering and compensation, such as range cell migration compensation (RCMC), in the frequency domain. The most commonly

| Device | C66x DSP Cores | ARM Cores | FFTC Accelerators | JESD204B & DFE | FFTs per sec (8192-pt FFT) | GFLOPS | SoC Power (100°C case temp) |
|--------------------|----------------|-----------|-------------------|---------------------------|----------------------------|--------|-----------------------------|
| TMS320C6657 | 2 | – | – | – | 8,000 | 10 | 4–5 W |
| TMS320C6670 | 4 | – | 3 | – | 214,000 | 125 | 9–13 W |
| TMS320C6678 | 8 | – | – | – | 32,000 | 40 | 20–22 W |
| 66AK2H06 | 4 | 2 | – | – | 16,000 | 20 | 14–18 W |
| 66AK2H12 | 8 | 2 | – | – | 32,000 | 40 | 18–22 W |
| 66AK2H14 | 8 | 2 | – | – | 32,000 | 40 | 19–24 W |
| 66AK2L06 | 4 | 2 | 2 | 4× JESD204B 4 TXRX DFE | 148,000 | 90 | 6–12 W |
| TCI6636K2H | 8 | 4 | 4 | – | 296,000 | 180 | 19–26 W |
| TCI6638K2K | 8 | 4 | 6 | – | 428,000 | 250 | 20–28 W |

Table 2: KeyStone-based devices and FFT performance

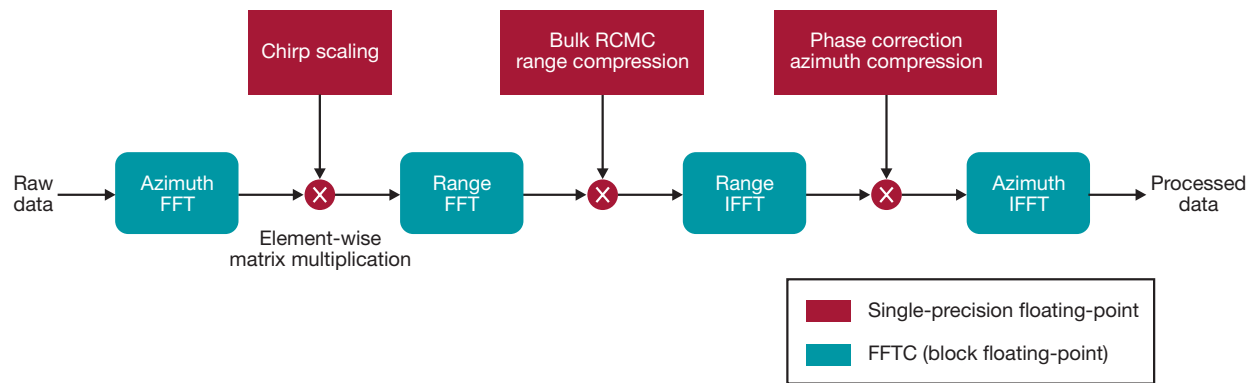


Figure 3: Chirp-scaling algorithm block diagram

employed SAR algorithms, such as the range Doppler algorithm (RDA), the chirp-scaling algorithm (CSA) and the wave number domain algorithm (or omega-k algorithm), all include the FFT and IFFT operations in both range and azimuth dimensions. In this paper, we use the CSA for analyzing the performance of the FFTC and quantifying the effect of the FFTC precision on the final SAR image quality. A high-level block diagram for the CSA [5] is shown in Figure 3. Matched filtering (also called compression) in both the range domain and the azimuth domain are performed in the frequency domain as shown in the figure. Range cell migration compensation in the CSA is implemented in three stages:

- The differential range cell migration (RCM) component is compensated in the first element-wise matrix multiplication using the chirp-scaling technique in the range-time and azimuth-frequency domain.
- The common or bulk component of RCM is compensated in the second element-wise matrix multiplication in the range-frequency and azimuth-frequency domain.
- The phase remaining after the previous two stages of RCMC is corrected in the third element-wise matrix multiplication.

A SAR simulator based on the model shown in Figure 3 was built with a bit-accurate hardware model for the FFTC, allowing us to analyze the performance of the FFTC on the quality of final SAR output image, compared with the performance of a single-precision floating-point FFT implementation.

A raw data of size $N_r \times N_a$ (the input to the SAR algorithm) is a collection of complex baseband samples, corresponding to N_a radar echoes (or azimuth samples), where each radar echo consists of N_r range-domain samples. The SAR algorithm that operates on a raw data of size $N_r \times N_a$ requires high-performance and high-throughput FFT/IFFT operations, specifically:

- N_r times N_a -point FFT and IFFT in the azimuth FFT/IFFT block
- N_a times N_r -point FFT and IFFT in the range FFT/IFFT block

Our performance evaluation includes several representative values of N_r and N_a (see Table 5 on page 9).

SAR system parameters

The SAR signal chain in the simulation includes the transmit signal (linear FM chirp), the antenna pattern, the point target model/channel and all of

the SAR signal processing. The test cases and associated system parameters for both aircraft and satellite systems used in the simulations are shown below in Table 3.

These representative SAR system parameters are taken from [4]. Test case 1 and Test case 2 are typical aircraft SAR systems with 50 and 100 MHz of system bandwidth, and 100 and 600 Hz of pulse repetition frequency (PRF), respectively. Test Case 3 is the system parameter set for RADARSAT-1, which has 30.11 MHz of system bandwidth and 1256.98 Hz of PRF. For each test case, three different squint angles are tested to explore performance sensitivity as a function of squint angle.

When simulated raw data is used in the performance analysis, it is based on the 2D SAR signal model detailed in [6]. An azimuth-direction antenna pattern based on following raised-cosine model is used:

$$\rho(\theta_r, \omega) = \frac{1}{2} + \frac{1}{2} \cos(\pi(\theta_r - \theta_{sq}) / \phi_d(\omega))$$

where θ_n is the incident angle for the n-th point target, θ_{sq} is the squint angle of the SAR system, and the divergence beam width ϕ_d is determined by the lateral antenna length as follows:

$$\phi_d(\omega) = \sin^{-1}(\lambda/D_a).$$

Performance comparison using point target analysis

In this section, we perform point target analysis to systematically evaluate the impact of the FFTC on the quality of the SAR output image. This analysis is performed on the impulse response function (IRF) of the SAR system that covers the end-to-end SAR signal chain. The point target analysis is based on simulated point-target raw data to avoid undesired effects such as clutter backscattering, noise, local reflection and incomplete calibration. More details on point target analysis can be found in [4].

| Parameter | Symbol | Test Case 1 Aircraft 50 MHz | Test Case 2 Aircraft 100 MHz | Test Case 3 RADARSAT-1 | Units |
|----------------------------------|---------------|--------------------------------|---------------------------------|---------------------------|--------------|
| Transmitted pulse duration | T_r | 2.5 | 10 | 41.74 | μ s |
| Range FM rate | K_r | 20 | 10 | 0.72135 | MHz/ μ s |
| Signal bandwidth | B | 50 | 100 | 30.11 | MHz |
| Baseband sampling rate | F_r | 60 | 120 | 32.32 | Msp/s |
| Radar center frequency | f_c | 5.3 | 9.4 | 5.3 | GHz |
| Effective radar velocity | V_r | 150 | 250 | 7062 | m/s |
| Antenna length | D_a | 4 | 1 | 15 | m |
| Pulse repetition frequency (PRF) | F_a | 100 | 600 | 1256.98 | Hz |
| Slant range of scene center | R_c | 20 | 30 | 100 | km |
| Squint angle | θ_{sq} | 0, 2, 4 | 0, 4, 8 | 0, -2, -4 | degree |

Table 3: Test cases for SAR performance evaluation

In the analysis, a scenario of nine point targets on a grid, separated by 500 m in both range and azimuth direction, is selected. After processing the simulated raw data with the CSA, each target on the compressed SAR image is examined, as shown in Figure 4, more specifically:

1. Applying 2D interpolation to produce more details of the peak profile. For each point target a 64×64 pixel image around the peak for the target point was interpolated in the analysis. An interpolation technique based on zero padding in frequency domain can be applied. More care has to be taken to signals with skewed spectrum, especially in non-zero squint cases.
2. Measuring the three profile metrics (see below) on each point target in both range and azimuth domains.

Performance metrics

The following three performance metrics are measured for each range-domain and azimuth-domain profile for every compressed point target (see Figures 5 and 6 on the following page). In

each case, the measurement is made using both the FFTC model and the SP floating-point FFT implementation for comparison purposes.

- Impulse response width (IRW): the width of the main lobe of the impulse response, measured at 3 dB below the peak value
- Peak side lobe ratio (PSLR): ratio between the height of the largest side lobe and the height of the main lobe
- Integrated side lobe ratio (ISLR), defined as:

$$ISLR = 10 \log_{10} \left\{ \frac{P_{total} - P_{main}}{P_{main}} \right\}$$

where P_{total} is the total power measured across the whole range of interest in the time domain, and P_{main} is the power of the main lobe. The main lobe for the ISLR is typically defined by the time domain samples corresponding to $\alpha \cdot IRW$ ($\alpha = 2.25$ is used throughout the analysis).

The IRW directly determines the resolution of the SAR image in each direction, since it is not possible to distinguish two different targets within the IRW in the compressed data. The side lobe metrics (PSLR and ISLR) are important measures since

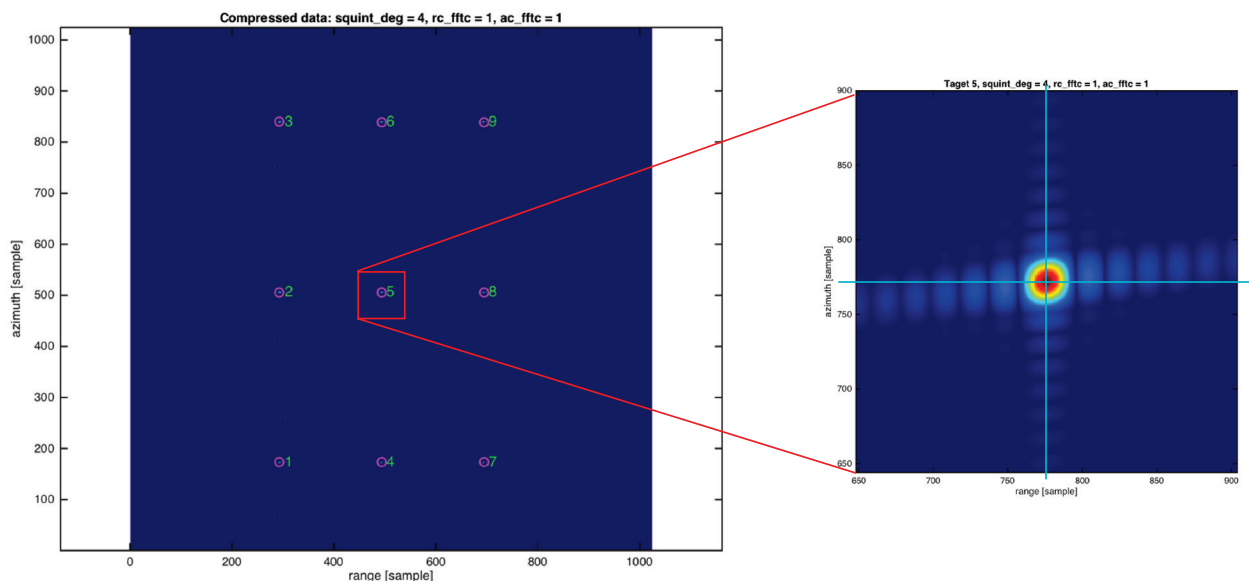


Figure 4: Point target analysis for nine point targets (Test case 1 with 4 degrees of squint angle).

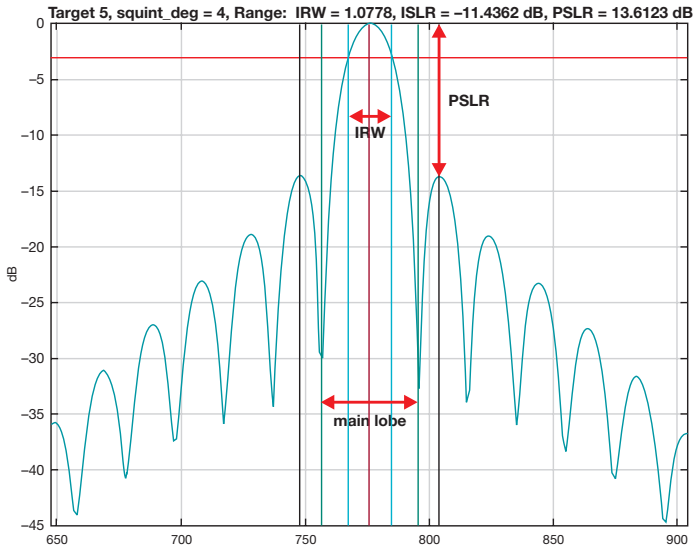


Figure 5: Point target analysis: range profile (Target 5 in Test case 1 with 4 degrees of squint angle)

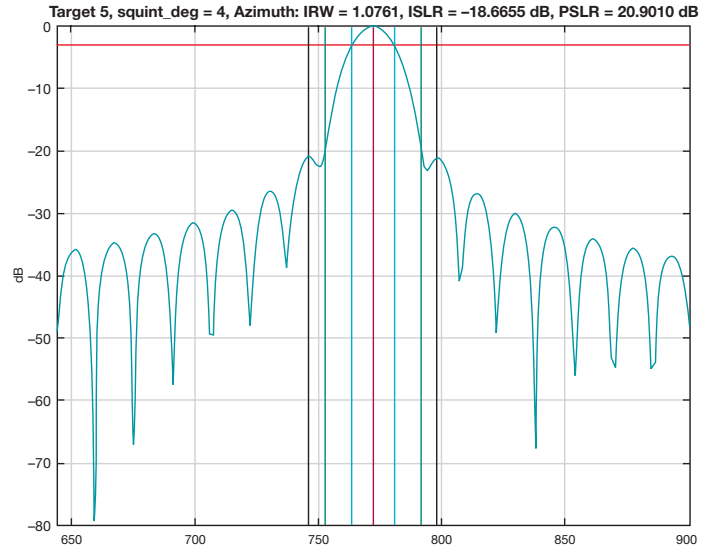


Figure 6: Point target analysis: azimuth profile (Target 5 in Test case 1 with 4 degrees of squint angle)

they characterize how well the SAR system works in non-ideal situations where a target with a weak radar cross-section (RCS) or reflection coefficient may be buried under the side lobe of a neighboring target with a strong RCS. Lower ISLR corresponds to a higher quality image produced by the SAR system.

Performance comparison

Table 4 summarizes the point target analysis for Test case 1 (aircraft 50 MHz) with 4 degrees of squint angle in range profile and azimuth profile. There are two columns for each performance metric, comparing the results with FFTC and the SP floating-point FFT. The results show that there is no

| Target index | Range profile | | | | | | Azimuth profile | | | | | |
|--------------------|---------------|--------|-----------|----------|-----------|---------|-----------------|--------|-----------|----------|-----------|---------|
| | IRW [sample] | | ISLR [dB] | | PSLR [dB] | | IRW [sample] | | ISLR [dB] | | PSLR [dB] | |
| | FFTC | FP | FFTC | FP | FFTC | FP | FFTC | FP | FFTC | FP | FFTC | FP |
| 1 | 1.0777 | 1.0777 | -11.4341 | -11.4344 | 13.6147 | 13.6148 | 1.0754 | 1.0754 | -18.7781 | -18.7780 | 21.1681 | 21.1671 |
| 2 | 1.0778 | 1.0778 | -11.4313 | -11.4319 | 13.5234 | 13.5238 | 1.0788 | 1.0788 | -18.5369 | -18.5376 | 20.9912 | 20.9904 |
| 3 | 1.0777 | 1.0777 | -11.4270 | -11.4272 | 13.5783 | 13.5783 | 1.0794 | 1.0794 | -18.6150 | -18.6154 | 21.0503 | 21.0513 |
| 4 | 1.0780 | 1.0780 | -11.4332 | -11.4336 | 13.5786 | 13.5786 | 1.0769 | 1.0769 | -18.6489 | -18.6491 | 21.0417 | 21.0420 |
| 5 | 1.0778 | 1.0779 | -11.4362 | -11.4366 | 13.6123 | 13.6129 | 1.0761 | 1.0761 | -18.6655 | -18.6658 | 20.9010 | 20.9001 |
| 6 | 1.0776 | 1.0776 | -11.4266 | -11.4271 | 13.5289 | 13.5292 | 1.0815 | 1.0815 | -18.4485 | -18.4490 | 20.9634 | 20.9631 |
| 7 | 1.0791 | 1.0791 | -11.4317 | -11.4320 | 13.5549 | 13.5551 | 1.0809 | 1.0809 | -18.4044 | -18.4046 | 20.9004 | 20.8998 |
| 8 | 1.0796 | 1.0796 | -11.4381 | -11.4384 | 13.5884 | 13.5888 | 1.0767 | 1.0767 | -18.6062 | -18.6063 | 20.8183 | 20.8178 |
| 9 | 1.0794 | 1.0794 | -11.4331 | -11.4334 | 13.6262 | 13.6265 | 1.0791 | 1.0791 | -18.4336 | -18.4345 | 20.7891 | 20.7896 |
| Maximum difference | 0.0000 | | 0.0005 | | 0.0006 | | 0.0000 | | 0.0009 | | 0.0010 | |

Table 4: Comparison of FFTC and SP floating-point FFT using point target analysis for Test case 1 with 4 degrees of squint angle

significant difference in all three metrics between the FFTC and the SP floating-point FFT. The last row of the table contains the maximum difference for each metric over the nine point targets. The maximum difference in ISLR and PSLR in the range domain profiles are 0.0005 dB and 0.0006 dB, respectively; in the azimuth domain, they are 0.0009 dB and 0.001 dB, respectively. These differences are negligible, and it can be concluded that there is no tangible difference in SAR image quality between the two FFT implementations.

Table 5 summarizes all results of the point target analysis for the three test cases:

- Test case 1 (aircraft 50 MHz) with 0, 4, and 8 degrees of squint angles, and 1024 × 1024 raw data size.
- Test case 2 (aircraft 100 MHz) with 0, 2, and 4 degrees of squint angles, and 8192 × 4096 raw data size.
- Test case 3 (RADARSAT-1), with 0, -2, and -4 degrees of squint angles, 8192 × 4096 raw data size.

Table 5 shows the maximum difference for each performance metric (over nine point targets). For each aircraft/satellite test case (further tested with three different squint angles), FFTC has virtually no

performance impact on the final SAR image quality. When compared to floating-point FFT, the difference in SAR image quality is less than 0.0015 dB in ISLR.

Performance comparison on output images

As another simple performance metric, we use peak SNR to quantify the difference between the two SAR output images: the first with FFTC and the second with SP floating-point FFT (as reference image). The peak SNR is defined as follows:

$$PSNR(X, Y) = \frac{\text{peak}(Y)}{MSE(X, Y)} = \frac{\max_{n,m} |y_{n,m}|^2}{\text{mean}_{n,m} |x_{n,m} - y_{n,m}|^2}$$

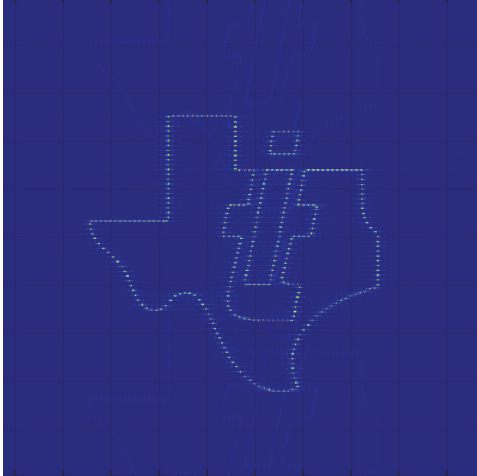
where X and Y are complex matrices, each represent one of two SAR output images. X and Y consist of $x_{n,m}$ and $y_{n,m}$ elements, respectively.

Simulated raw data (1024 × 1024)

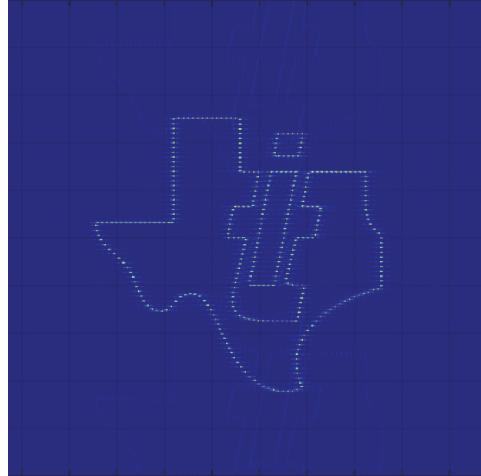
The first example (Figure 7 on the following page) shows the two SAR output images for Test case 1 (aircraft 50 MHz) with an input of 1024 × 1024 simulated raw data for more than 300-point targets.

| Test case ($N_r \times N_a$) | Squint angle [degree] | Range profile | | | Azimuth profile | | |
|-----------------------------------|--------------------------|---------------|-----------|-----------|-----------------|-----------|-----------|
| | | IRW [sample] | ISLR [dB] | PSLR [dB] | IRW [sample] | ISLR [dB] | PSLR [dB] |
| Test Case 1 (1024 × 1024) | 0 | 0.0000 | 0.0015 | 0.0005 | 0.0000 | 0.0015 | 0.0017 |
| | 4 | 0.0000 | 0.0005 | 0.0006 | 0.0000 | 0.0009 | 0.0010 |
| | 8 | 0.0000 | 0.0004 | 0.0003 | 0.0000 | 0.0004 | 0.0012 |
| Test Case 2 (4096 × 8192) | 0 | 0.0000 | 0.0009 | 0.0005 | 0.0000 | 0.0013 | 0.0018 |
| | 2 | 0.0000 | 0.0005 | 0.0005 | 0.0000 | 0.0007 | 0.0017 |
| | 4 | 0.0000 | 0.0007 | 0.0005 | 0.0002 | 0.0011 | 0.0002 |
| Test Case 3 (4096 × 4096) | 0 | 0.0000 | 0.0007 | 0.0003 | 0.0000 | 0.0007 | 0.0021 |
| | -2 | 0.0000 | 0.0008 | 0.0004 | 0.0000 | 0.0010 | 0.0012 |
| | -4 | 0.0000 | 0.0005 | 0.0005 | 0.0000 | 0.0009 | 0.0024 |

Table 5: Maximum performance difference (over nine point targets) between FFTC and floating-point FFT for all test cases



(a) When using FFTC



(b) When using floating-point FFT

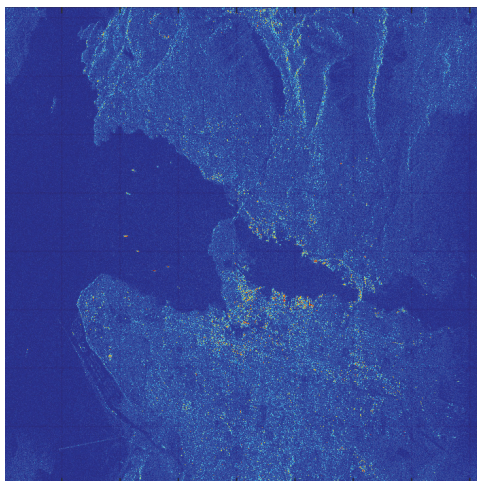
Figure 7: Performance for 1024×1024 SAR data with simulated raw data (Test case 1)

The majority of point targets on the horizontal and vertical lines of the logo are separated by 10 m. The measured PSNR is 94 dB, and no real difference is observed in SAR image quality between the two output images.

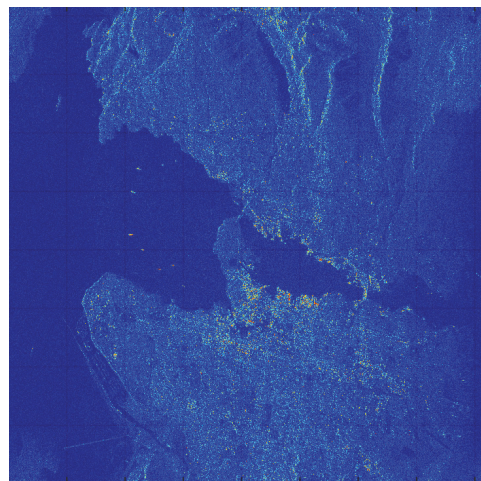
an accompanying CD). 4096×4096 raw data is processed for the two analysis methods (FFTC and floating-point FFT). The measured PSNR = 107 dB. Note that the Doppler centroid frequency is estimated using the same raw data and exploited in the CSA algorithm. From the two examples, it is clear that use of the FFTC over the floating-point FFT has no significant difference on the final SAR image quality.

RADARSAT-1 raw data (4096×4096)

The second example (Figure 8) uses the measured raw data of RADARSAT-1 (that is provided in [4] in



(a) When using FFTC



(b) When using floating-point FFT on C66x

Figure 8: Performance for 4096×4096 SAR measured data of RADARSAT-1 (Test case 3)

[Provided courtesy of MacDonald, Dettwiler and Associates Ltd. (MDA). Copyright: RADARSAT Data © Canadian Space Agency/Agence Spatiale Canadienne (2002). All Rights Reserved]

Conclusion

The high-performance FFTC was applied to high-end SAR applications and its performance was evaluated through point target analysis on the compressed SAR image as well as by comparing the final output images for various representative use cases for both air-borne and space-borne SAR systems. For all test cases, the results show that the FFTC produces a SAR output image with quality indistinguishable from that of a floating-point FFT. The FFTC allows the heavy computation load of 2D FFT used in many high-performance radar signal applications to be offloaded. As shown in the FFTC performance section, the high throughput of the FFTC, compared to implementing the floating-point FFT on DSP cores, improves the latency and performance of the radar application. The gained performance of using the FFTC engines on TI SoCs allows radar system designers to implement high-performance systems achieving low latency, high accuracy within the difficult size, weight and power constraints imposed by real-world constraints.

References

- [1] S. Aridhi and S. Narnakaje, Texas Instruments white paper, "**Optimizing Synthetic Aperture Radar design with TI's integrated 66AK2L06 SoC**"
- [2] D. Wang, M. Ali, and E. Blinka, Texas Instruments white paper "**Synthetic Aperture Radar (SAR) Implementation on a TMS320C6678 Multicore DSP**"
- [3] **Fast Fourier Transform Coprocessor (FFTC) for KeyStone II Devices User's Guide (Rev. A).**
- [4] I. G. Cumming and F. H. Wong, *Digital Processing of Synthetic Aperture Radar Data: Algorithms and Implementation*, Artech House, 2005.
- [5] R. K. Raney, H. Runge, R. Bamler, I. G. Cumming, and F. H. Wong, "Precision SAR processing using chirp scaling," *IEEE Trans. on Geoscience and Remote Sensing*, July 1994.
- [6] M. Soumekh, *Synthetic Aperture Radar Signal Processing with MATLAB Algorithms*, Wiley, 1999.

Important Notice: The products and services of Texas Instruments Incorporated and its subsidiaries described herein are sold subject to TI's standard terms and conditions of sale. Customers are advised to obtain the most current and complete information about TI products and services before placing orders. TI assumes no liability for applications assistance, customer's applications or product designs, software performance, or infringement of patents. The publication of information regarding any other company's products or services does not constitute TI's approval, warranty or endorsement thereof.

KeyStone is a trademark of Texas Instruments. All other trademarks are the property of their respective owners.

IMPORTANT NOTICE

Texas Instruments Incorporated and its subsidiaries (TI) reserve the right to make corrections, enhancements, improvements and other changes to its semiconductor products and services per JESD46, latest issue, and to discontinue any product or service per JESD48, latest issue. Buyers should obtain the latest relevant information before placing orders and should verify that such information is current and complete. All semiconductor products (also referred to herein as "components") are sold subject to TI's terms and conditions of sale supplied at the time of order acknowledgment.

TI warrants performance of its components to the specifications applicable at the time of sale, in accordance with the warranty in TI's terms and conditions of sale of semiconductor products. Testing and other quality control techniques are used to the extent TI deems necessary to support this warranty. Except where mandated by applicable law, testing of all parameters of each component is not necessarily performed.

TI assumes no liability for applications assistance or the design of Buyers' products. Buyers are responsible for their products and applications using TI components. To minimize the risks associated with Buyers' products and applications, Buyers should provide adequate design and operating safeguards.

TI does not warrant or represent that any license, either express or implied, is granted under any patent right, copyright, mask work right, or other intellectual property right relating to any combination, machine, or process in which TI components or services are used. Information published by TI regarding third-party products or services does not constitute a license to use such products or services or a warranty or endorsement thereof. Use of such information may require a license from a third party under the patents or other intellectual property of the third party, or a license from TI under the patents or other intellectual property of TI.

Reproduction of significant portions of TI information in TI data books or data sheets is permissible only if reproduction is without alteration and is accompanied by all associated warranties, conditions, limitations, and notices. TI is not responsible or liable for such altered documentation. Information of third parties may be subject to additional restrictions.

Resale of TI components or services with statements different from or beyond the parameters stated by TI for that component or service voids all express and any implied warranties for the associated TI component or service and is an unfair and deceptive business practice. TI is not responsible or liable for any such statements.

Buyer acknowledges and agrees that it is solely responsible for compliance with all legal, regulatory and safety-related requirements concerning its products, and any use of TI components in its applications, notwithstanding any applications-related information or support that may be provided by TI. Buyer represents and agrees that it has all the necessary expertise to create and implement safeguards which anticipate dangerous consequences of failures, monitor failures and their consequences, lessen the likelihood of failures that might cause harm and take appropriate remedial actions. Buyer will fully indemnify TI and its representatives against any damages arising out of the use of any TI components in safety-critical applications.

In some cases, TI components may be promoted specifically to facilitate safety-related applications. With such components, TI's goal is to help enable customers to design and create their own end-product solutions that meet applicable functional safety standards and requirements. Nonetheless, such components are subject to these terms.

No TI components are authorized for use in FDA Class III (or similar life-critical medical equipment) unless authorized officers of the parties have executed a special agreement specifically governing such use.

Only those TI components which TI has specifically designated as military grade or "enhanced plastic" are designed and intended for use in military/aerospace applications or environments. Buyer acknowledges and agrees that any military or aerospace use of TI components which have **not** been so designated is solely at the Buyer's risk, and that Buyer is solely responsible for compliance with all legal and regulatory requirements in connection with such use.

TI has specifically designated certain components as meeting ISO/TS16949 requirements, mainly for automotive use. In any case of use of non-designated products, TI will not be responsible for any failure to meet ISO/TS16949.

Products

| | |
|------------------------------|--|
| Audio | www.ti.com/audio |
| Amplifiers | amplifier.ti.com |
| Data Converters | dataconverter.ti.com |
| DLP® Products | www.dlp.com |
| DSP | dsp.ti.com |
| Clocks and Timers | www.ti.com/clocks |
| Interface | interface.ti.com |
| Logic | logic.ti.com |
| Power Mgmt | power.ti.com |
| Microcontrollers | microcontroller.ti.com |
| RFID | www.ti-rfid.com |
| OMAP Applications Processors | www.ti.com/omap |
| Wireless Connectivity | www.ti.com/wirelessconnectivity |

Applications

| | |
|-------------------------------|--|
| Automotive and Transportation | www.ti.com/automotive |
| Communications and Telecom | www.ti.com/communications |
| Computers and Peripherals | www.ti.com/computers |
| Consumer Electronics | www.ti.com/consumer-apps |
| Energy and Lighting | www.ti.com/energy |
| Industrial | www.ti.com/industrial |
| Medical | www.ti.com/medical |
| Security | www.ti.com/security |
| Space, Avionics and Defense | www.ti.com/space-avionics-defense |
| Video and Imaging | www.ti.com/video |

TI E2E Community

e2e.ti.com